SOILS AND FOUNDATIONS Vol. 51, No. 1, 1–10, Feb. 2011
Japanese Geotechnical Society

APPROXIMATE NUMERICAL ANALYSIS OF A LARGE PILED RAFT FOUNDATION

PASTSAKORN KITIYODOM[i], TATSUNORI MATSUMOTO[ii] and RYUUICHI SONODA[iii]

ABSTRACT

An approximate method of analysis has been developed to estimate the settlement and load distribution of large piled raft foundations. In the method the raft is modelled as a thin plate, and the piles and the soil are treated as interactive springs. Both the resistances of the piles as well as the raft base are incorporated into the model. Pile-soil-pile interaction, pile-soil-raft interaction and raft-soil-raft interaction are taken into account based on Mindlin's solutions. The proposed method makes it possible to solve problems of large non-uniformly arranged piled rafts in a time-saving way using a PC. The method can also be used for the deformation analysis of pile groups by setting the soil resistance at the raft base equal to zero. The validity of the proposed method is verified through comparisons with existing solutions. Two case studies on settlement analyses of a free-standing pile group and a large piled raft are presented. In the analyses, applicability of the equivalent pier concept is also examined and discussed. The computed settlements compare favourably with the field measurements.

Key words: large piled raft, pile, pile group, pile load test, simplified deformation analysis, site monitoring (**IGC**: C7/C8/E4)

INTRODUCTION

Piled raft foundations have been used to support a variety of structures, and they are now widely recognized as one of the most economical methods of foundation systems since Burland et al. (1977) presented the concept of 'settlement reducers'. This type of foundation has been used in Japan since 1980s (for example, Kakurai, 2003).

As a preliminary routine design tool of piled raft foundations subjected to vertical, horizontal and moment loading as well as free-field ground movements, a computer program PRAB (Piled Raft Analysis with Batter piles) has been developed by Kitiyodom and Matsumoto (2002, 2003) and Kitiyodom et al. (2005).

In PRAB a hybrid model, in which the flexible raft is modelled as a thin plate, the piles as elastic beams and the soil is treated as interactive springs, is employed. Both the vertical and horizontal resistances of the piles as well as the raft base are incorporated into the model (*see* Fig. 1(a)). Pile-soil-pile, pile-soil-raft and raft-soil-raft interactions are taken into account based on Mindlin's solutions (Mindlin, 1936) for both vertical and horizontal forces.

In this work, the approach described previously by the authors is modified, in order to make it possible to solve problems of large non-uniformly arranged piled raft foundations in a time-saving way using a PC. Instead of

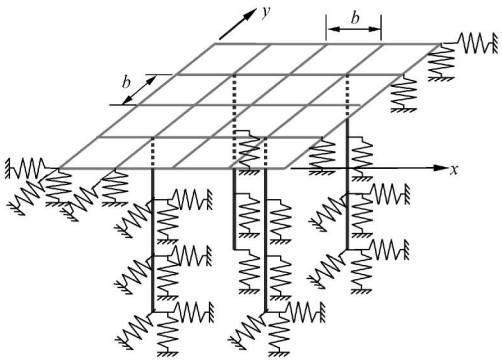

(a) Plate-beam-spring model used in PRAB

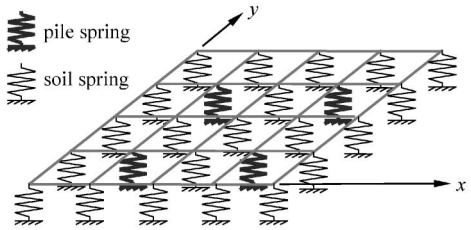

(b) Plate-spring model used in PRABS

Fig. 1. Plate-spring modelling of a piled raft foundation

[i] Senior Engineer, Geotechnical & Foundation Engineering Co., Ltd., Bangkok, Thailand (pastsakorn_k@gfe.co.th).
[ii] Professor, Graduate School of Natural Science and Technology, Kanazawa University, Ishikawa, Japan.
[iii] Doctoral Student, ditto.
The manuscript for this paper was received for review on November 16, 2009; approved on August 30, 2010.
Written discussions on this paper should be submitted before September 1, 2011 to the Japanese Geotechnical Society, 4-38-2, Sengoku, Bunkyo-ku, Tokyo 112-0011, Japan. Upon request the closing date may be extended one month.

modelling pile as elastic beams, each pile is modelled as an interactive spring with appropriate stiffness (*see* Fig. 1(b)).

Similar methods representing raft as a thin plate, soil and piles as springs were also proposed by other researchers, e.g., Anagnostopoulos and Geogiadis (1998), Russo (1998), Yamashita et al. (1998) and Kim et al. (2001). Iterative procedure is required in Anagnostopoulos and Geogiadis (1998) and Yamashita et al. (1998). The interaction between piles and raft is neglected as the Winkler spring model is used in Kim et al. (2001). In Russo (1998), the Boussinesq's point load solution is used to calculate the displacement occurring at each raft node, due to the contact pressure developed at the interface of each raft element, while pile-soil-pile interaction factors are computed from the approximate solutions. In the simplified PRAB, called PRABS hereafter, no iterative procedure is required, and pile-soil-pile, pile-soil-raft and raft-soil-raft interactions are calculated based on Mindlin's solutions.

The validity of PRABS is examined by comparisons with existing solutions. Finally, comparisons are made between the field measurements of a full-scale piled raft foundation and those computed from the proposed method. Moreover, as an alternative solution to reduce the computation time, the concept of the equivalent pier in which a number of piles are modelled as an equivalent pier was employed and discussed.

METHOD OF ANALYSIS

Numerical Method

In PRABS, the raft is modelled as a thin elastic plate, while the piles and the soil are treated as interactive springs attached to the raft as shown in Fig. 1(b).

The vertical soil springs, k_R, at the raft nodes are estimated by Eq. (1).

$$k_R = \frac{4\bar{G}_s a}{1-\bar{\nu}_s} \times \frac{1}{\{1-\exp(-h/2a)\}} \tag{1}$$

where h is the finite soil depth and a is the equivalent radius of the raft element. For a square raft element with a width of d, a can be estimated as $a = d/\sqrt{\pi}$. $\bar{G}_s$ and $\bar{\nu}_s$ are the equivalent shear modulus and the equivalent Poisson's ratio of the whole soil which can be determined following Fraser and Wardle (1976).

$$\bar{G} = \frac{\bar{E}_s^*}{2(1+\bar{\nu}_s)} \tag{2}$$

$$\bar{\nu}_s = \sum_{i=1}^{n} \nu_{s(i)} \Delta I_i / \Delta I_{\text{total}} \tag{3}$$

where $\bar{E}_s^*$ is the equivalent Young's modulus for the whole soil given by Eq. (4).

$$\frac{1}{\bar{E}_s^*} = \sum_{i=1}^{n} \frac{1}{E_{s(i)}^*} \Delta I_i / \Delta I_{\text{total}} \tag{4}$$

where $E_{s(i)}^*$ is the equivalent Young's modulus for the soil layer number i given by Eq. (5).

$$E_{s(i)}^* = E_{s(i)}/(1-\nu_{s(i)}^2) \tag{5}$$

where $E_{s(i)}$ and $\nu_{s(i)}$ are the Young's modulus and the Poisson's ratio for soil layer number i in the n-layered system. ΔI_i and ΔI_{total} in Eqs. (3) and (4) are the differences between the vertical settlement influence factors at different soil depths which can be determined by Eqs. (6) and (7).

$$\Delta I_i = I(z_{\text{top}}^i) - I(z_{\text{bottom}}^i) \tag{6}$$

$$\Delta I_{\text{total}} = I(0) - I(h) \tag{7}$$

where z_{top}^i and z_{bottom}^i are the depths below the surface of the top and bottom of layer number i. The vertical settlement influence factor I has been given by Harr (1966).

The pile spring stiffness can either be directly input into the program after obtaining it from another analysis (for example, the program PRAB), or else calculated from Eq. (8) following Randolph and Wroth (1978).

$$k_p = G_s r_0 = \frac{\dfrac{4}{\eta(1-\nu_s)} + \dfrac{2\pi\rho}{\zeta} \dfrac{\tanh(\mu L)}{\mu L} \dfrac{L}{r_0}}{1 + \dfrac{4}{\pi\lambda\eta(1-\nu_s)} \dfrac{\tanh(\mu L)}{\mu L} \dfrac{L}{r_0}} \tag{8}$$

in which $\zeta = \ln[2.5(L/r_0)\rho(1-\nu)]$; $(\mu L)^2 = [2/(\zeta\lambda)](L/r_0)^2$; $\rho = G_{L/2}/G_L$; $\lambda = E_p/G_L$; $\eta = 1$. L and r_0 are the length and the radius of the pile. $G_{L/2}$ and G_L are the soil shear modulus at the depth equal to half of the pile length and that at the depth equal to the pile length. E_p is the Young's modulus of the pile.

In all solutions presented herein, the pile spring stiffness has been computed using PRAB. The estimation of non-linear deformation of the foundations can be calculated by employing the bi-linear response of the soil and the pile springs.

Pile-soil-pile, pile-soil-raft and raft-soil-raft interactions are taken into account based on Mindlin's solutions. The interaction between the raft nodes is calculated directly using Mindlin's solutions. However, as each pile is modelled as a single spring, a point at some characteristic depth, $z = \xi L$, below the ground surface should be used to obtain the interaction between the pile and the raft nodes and the interaction between the pile nodes. In order to obtain an appropriate value for the parameter ξ, a parametric study has been carried out. The interaction factor, α, calculated using Mindlin's solutions with different characteristic depths is compared with the results calculated using PRAB in which the pile is modelled as a series of beam elements, and consider the interaction between each pile nodes. The interaction factor is defined as the ratio of the additional pile head displacement of the considered pile due to the effect of a neighbouring pile while both piles are subjected to vertical pile head load, to the pile head displacement of non-influenced single pile subjected to a vertical pile head load (*see* Fig. 2).

$$\alpha = \frac{\text{Additional settlement caused by adjacent pile}}{\text{Settlement of pile under its own load}} = \frac{w_1 - w_0}{w_0} \tag{9}$$

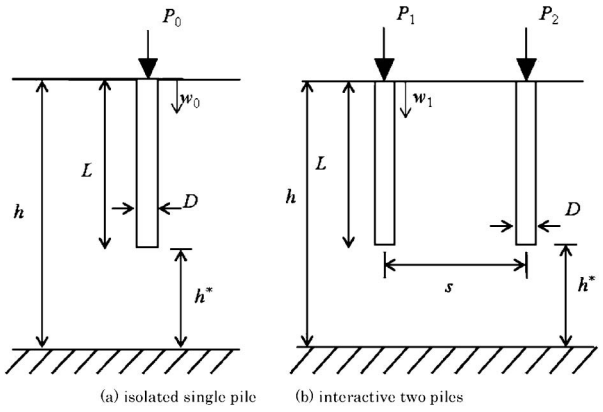

Fig. 2. Calculation of interaction factor, α, using PRAB

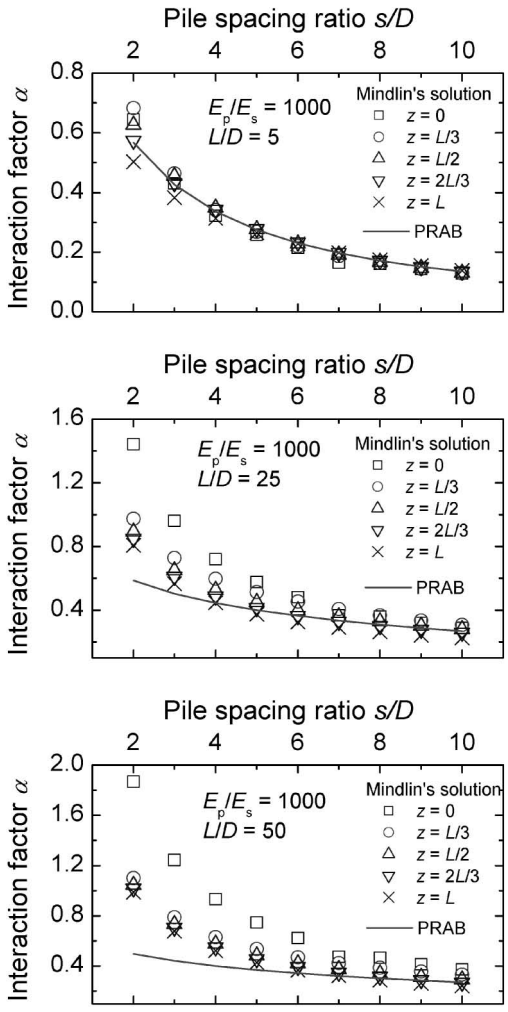

Fig. 3. Comparison of the interaction factors for various L/D

Figure 3 shows the influence of pile spacing between two piles embedded in a deep homogenous soil layer on the interaction factor, α, for three different pile slenderness ratios, L/D. The influence of pile spacing ratio, s/D, on the interaction factor is also shown in Fig. 4 for two different pile-soil stiffness ratios, E_p/E_s.

It can be seen from the figures that the interaction factors calculated using a characteristic depth of $2L/3$ shows a reasonable overall agreement especially for the cases of $L/D<25$ and $s/D>3$ with the results calculated using PRAB. So in the proposed method, the characteristic depth of $2L/3$ is employed in the calculation of pile-soil-pile and pile-soil-raft interactions. The validity of this assumption is examined through the comparisons with existing solutions and field measurements.

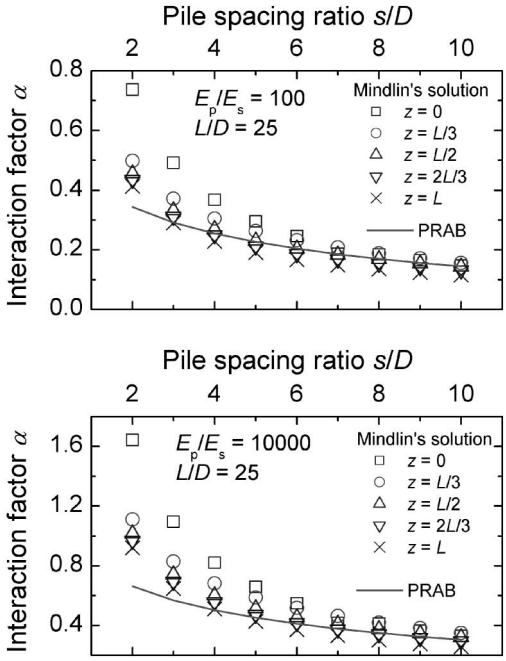

Fig. 4. Comparison of the interaction factors for various E_p/E_s

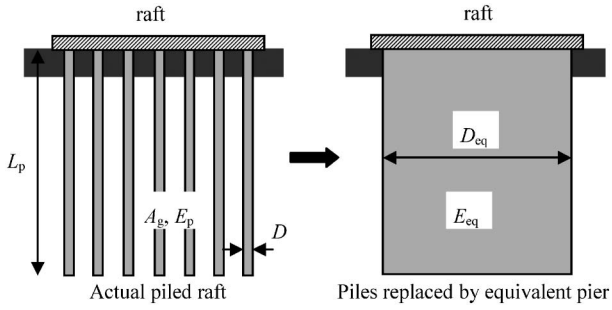

Fig. 5. Concept of equivalent pier method

Equivalent Pier Concept

For calculation relating to large structures supported by a number of pile groups, Poulos and Davis (1980) proposed the equivalent pier method. Horikoshi and Randolph (1999) employed this method to estimate the overall settlement of piled rafts. In this method, a number of piles are replaced by a single 'equivalent pier' as shown in Fig. 5.

As suggested by Randolph (1994), the diameter of the equivalent pier, D_{eq}, can be taken as

$$D_{eq} = 2\sqrt{A_g/\pi} \tag{10}$$

where A_g is the plan area of the pile group as a block.

Young's modulus of the equivalent pier, E_{eq}, is then calculated as

$$E_{eq} = E_s + (E_p - E_s)A_{tp}/A_g \quad (11)$$

where E_p is the Young's modulus of the pile, E_s the average Young's modulus of the soil penetrated by the piles, and A_{tp} is the total cross-sectional area of the piles in the group. Randolph and Clancy (1993) discussed the applicability of the equivalent pier method and proposed an appropriate parameter to categorize as

$$R = \sqrt{ns/L_p} \quad (12)$$

where n is the number of piles and s is the pile spacing. It was shown in their work that the equivalent pier approach was suitable for values of R less than 4 and certainly for values less than 2.

COMPARISONS WITH EXISTING SOLUTIONS

Raft Alone

For a square raft having a length of L_R subjected to an uniform vertical load, q, resting on a deep homogeneous layer, Fig. 6 compares the distributions of normalised settlement, S, contact pressure, p, and the bending moment, M_x, from PRABS, with those from the piled strip model (GARP) by Poulos (1994), and the finite element analysis by Hain and Lee (1978). It can be seen that there are good agreements among the solutions in all cases.

Piled Raft

Figure 7 shows the solutions for maximum settlement, S_{max}, of a uniformly loaded square raft supported by 64 piles, in a deep homogeneous elastic soil layer. The normalised maximum settlement is plotted as a function of the raft-soil stiffness ratio, K_R, for four different pile slenderness ratios, where

$$K_R = \frac{2E_R t^3 B_R(1-\nu_s^2)}{3\pi E_s L_R^4} \quad (13)$$

and E_R is the raft Young's modulus, t the raft thickness, and L_R and B_R are the raft dimensions.

The results calculated from PRABS are compared with those from GARP and the finite element analysis by Hain and Lee (1978).

Figures 8 and 9 show comparisons between the solutions for differential settlement and the proportion of

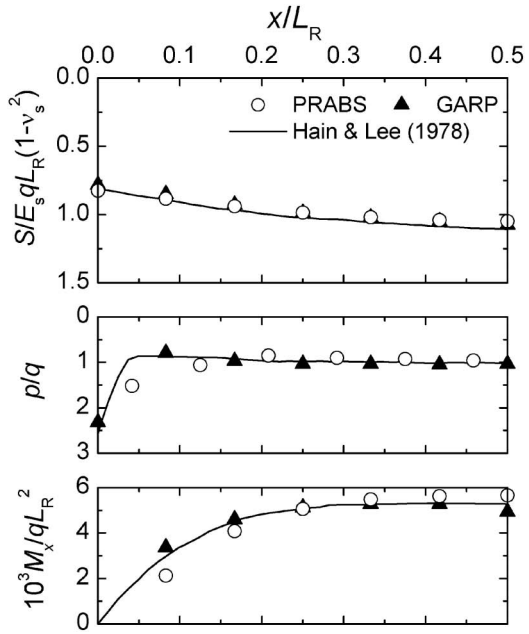

Fig. 6. Comparisons between solutions for uniformly loaded raft

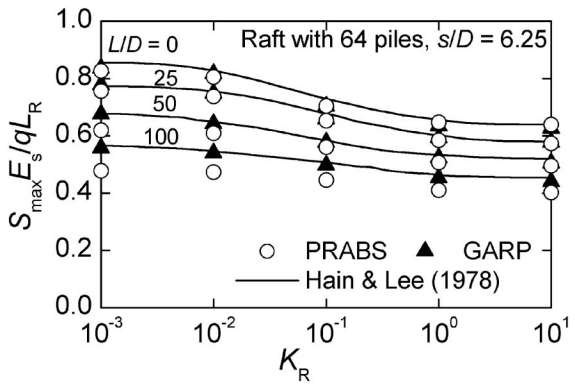

Fig. 7. Comparison between solutions for maximum settlement

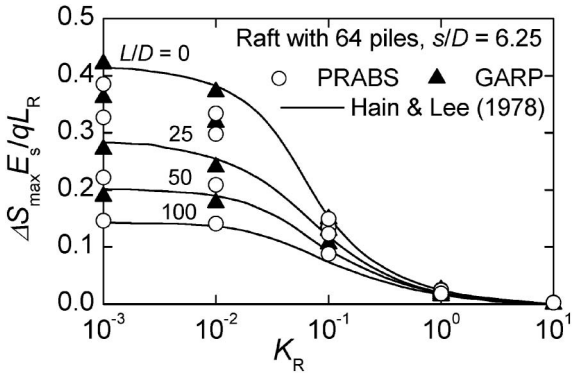

Fig. 8. Comparison between solutions for differential settlement

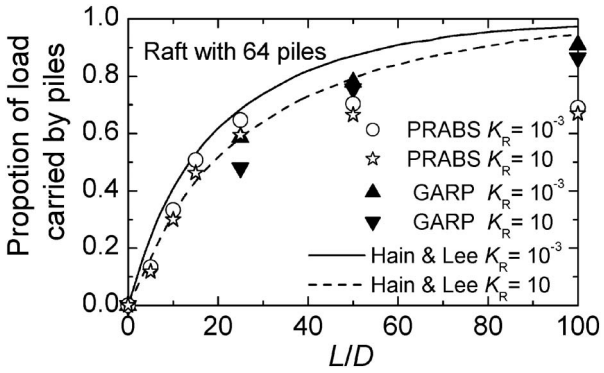

Fig. 9. Comparison between solutions for proportion of load carried by piles

load carried by the piles. Despite the approximations involved, PRABS can provide solutions of adequate accuracy for the settlement and pile load distribution within a piled raft with L/D less than 25 and s/D greater than 3 which are common for piled raft foundation employed in practice.

CASE STUDIES

Sonoda et al. (2009) have described the case of a large piled raft foundation for a commercial building called Amuplaza that was constructed in Kagoshima City, Kyushu, in 2003 to 2004. The building is 7-storied with a basement floor having a building area of 9000 m^2, a floor area of 50000 m^2, and a maximum height of 45 m (*see* Fig. 10). A piled raft foundation was employed for the building in a sandy ground to reduce the average settlement as well as the differential settlement. The building was constructed using a reverse construction method, in which construction of the superstructure (building) and the substructure (foundation) were constructed simultaneously, in order to reduce the construction period. Therefore the foundation was regarded as a free standing pile group without contribution of the raft resistance in earlier stages of construction, while the foundation behaved as a piled raft after the construction of the mat slab (raft) was completed. A static vertical pile load test was carried out at the construction site. Moreover, during the construction stage, settlements of the foundation and the water pressure beneath the raft were monitored.

A test pile was constructed additionally at a location indicated by 'star' symbol in Fig. 10. The test pile was a cast-in-situ concrete pile having a length of 32.0 m and a diameter of 1.0 m.

The programs PRAB and PRABS were employed to analyse the behaviour of the whole piled raft system. The analyses were carried out in two stages. The first stage was the deformation analysis in the stage of pile group where the raft resistance was not expected. The analysis in the stage of piled raft was carried out after the end of the first stage, considering the existence of the raft resistance. The stress conditions at the end of the first stage were used for the initial conditions in the second stage. Shear moduli of the soils at small strain, G_0, were derived by Sonoda et al. (2009) on the basis of SPT and PS-logging tests as shown in Fig. 11.

In order to determine the soil parameters appropriately, back-analysis of the vertical load test of the test pile was carried out using PRAB, prior to the analysis of the whole foundation. The test single pile and the ground were modelled as Fig. 12. Young's modulus of the pile $E_p = 2.27 \times 10^7$ kPa was employed. The maximum shaft friction, f_{max}, of each section obtained from the static vertical pile load test results was adopted in the back-analysis.

Figure 13 shows comparison of the analysed and measured load-settlement curves of the pile head and the pile base. Good matching was obtained if the shear modulus of the soil obtained from PS-logging was reduced by a factor of 2 for the soils surrounding the pile shaft and by a factor of 5 for the soil beneath the pile base. These reductions in the shear moduli of the soils may be reasonable, considering disturbance of the soils around the pile, and difference of strain levels between the pile load test

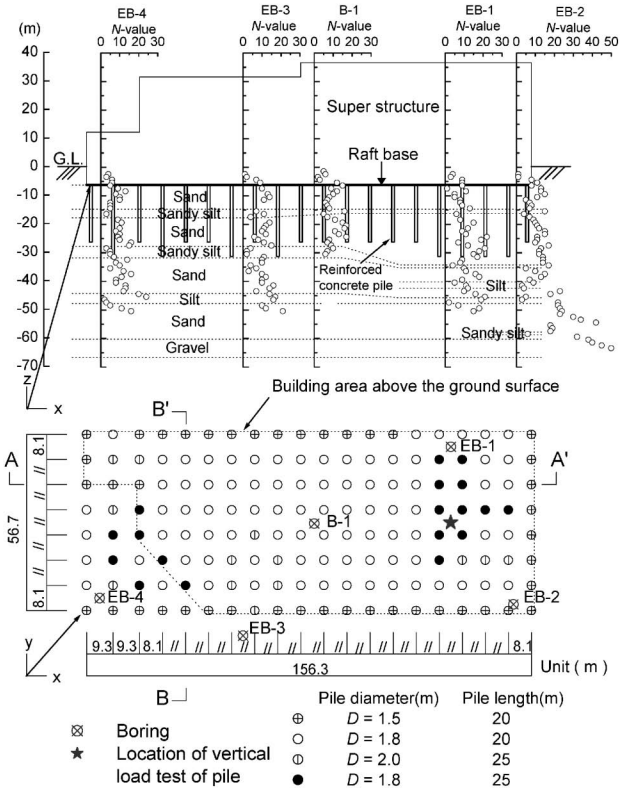

Fig. 10. Elevation view of building and arrangement of piles

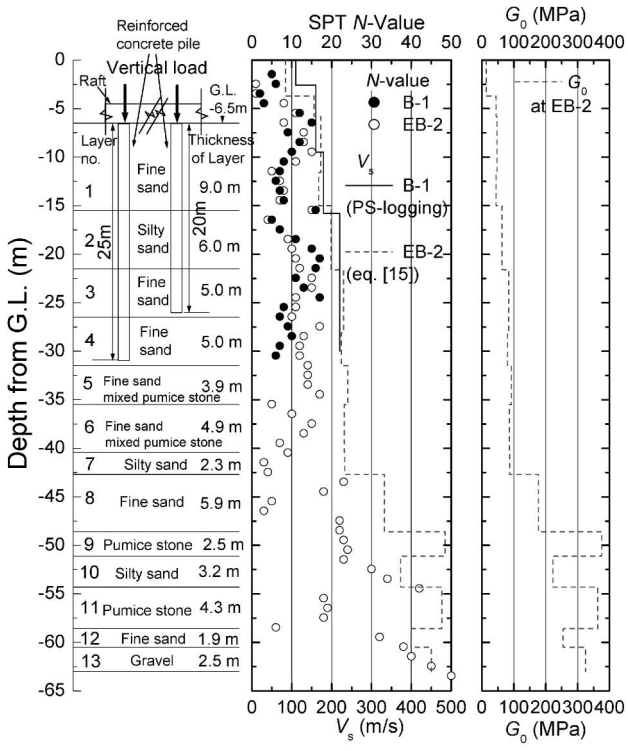

Fig. 11. Modelling of foundation and ground

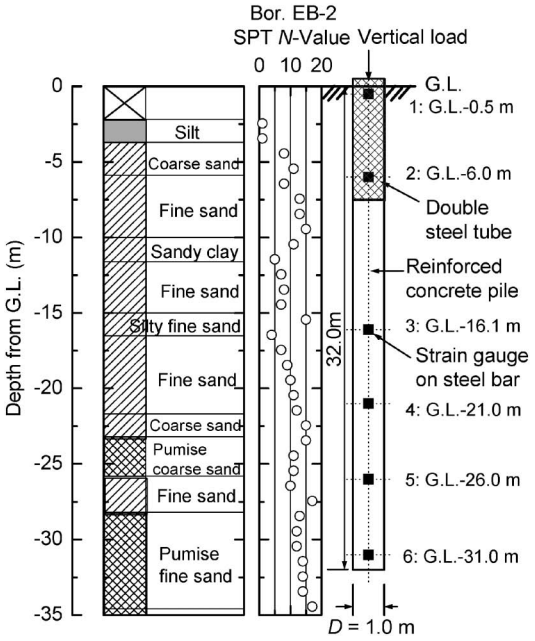

Fig. 12. Seating of test pile, and soil profile and SPT-*N* values obtained at borehole EB-2

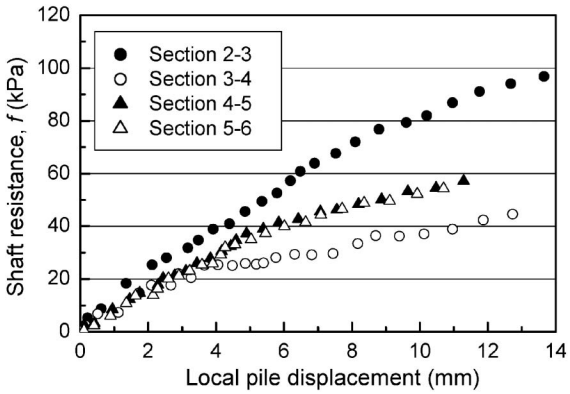

Fig. 14. Relationship between shaft resistance and local pile displacement

Table 1. Parameters for the calculation of load-settlement curves

Soil layer	Depth* (m)	G (kPa)	τ_f (kPa)	q (kPa)
1	6.5 to 15.5	51,840	99.5	
2	15.5 to 21.5	77,440	44.6	
3	21.5 to 26.5	77,440	54.3	900
4	26.5 to 31.5	77,440	54.3	900

* Ground level is at the depth = 6.5 m

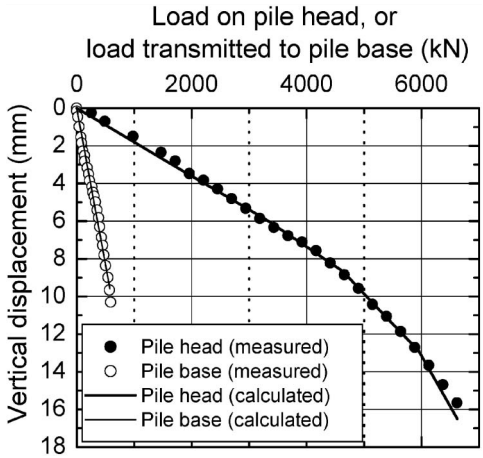

Fig. 13. Comparison of load-settlement curves of the test pile

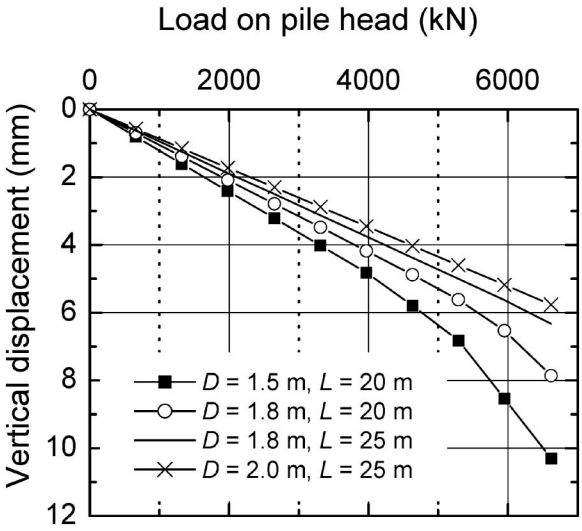

Fig. 15. Calculated load-settlement curves of construction pile from which pile spring stiffness used in PRABS is obtained

and PS-logging. Such reduction in the shear moduli of the soils around the pile are considered also in the post analysis of the whole foundation. In order to take into account the non-linear response, the value of the ultimate pile shaft resistance, τ_f, and the pile base bearing capacity, q, were set based on the measured values as shown in Fig. 14. Table 1 summarises the soil properties used in the matching analysis. These soil properties were also employed in the calculation of the stiffness values of the pile springs for the piles which have different configurations from the test pile. Figure 15 shows the calculated load-settlement curves for four different configuration piles which were constructed in the site. Note that pile spring stiffness used in PRABS is obtained from these curves.

The modelling of the foundation and the ground has been shown in Fig. 11. It was judged that the modelling of the ground to a depth of 63 m is needed when analysing such a large piled raft foundation because the influence of the wide length of the raft of 156 m reaches to deeper depths. Note here that SPT *N*-values for depths greater than 63 m were very large and the depth of 63 m was assumed to be a bed stratum.

For the analysis using PRAB with the equivalent pier concept, Fig. 16 shows the arrangement of the piles and the equivalent piers. Properties of the equivalent piers are summarised in Table 2. It can be seen that the values of R (defined in Eq. (5)) in all types of equivalent piers are less than 2.

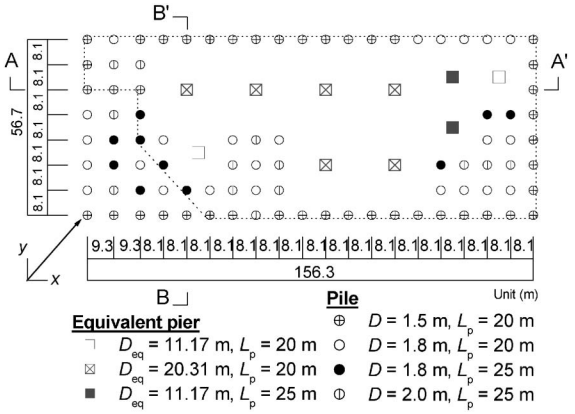

Fig. 16. Arrangement of piles and equivalent piers

Table 2. Properties of equivalent piers

Pier type	D_{eq} (m)	L_p (m)	E_{eq} (kPa)	R
1	11.17	20	2.51×10^6	1.27
2	20.31	20	1.76×10^6	1.90
3	11.17	25	2.51×10^6	1.14

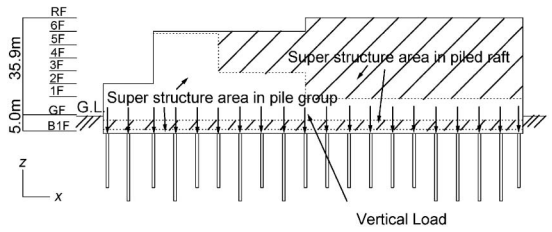

Fig. 17. Construction areas of superstructure in stages of pile group and piled raft

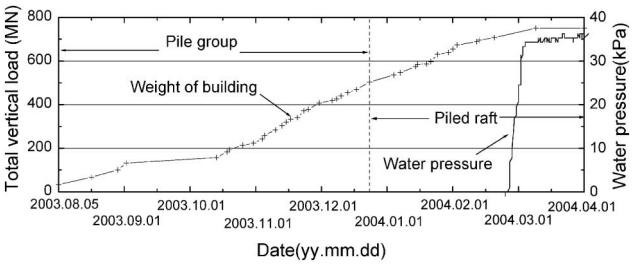

Fig. 18. Time histories of the total load from the building and measured water pressure at the raft base

The interaction factors and soil springs at the raft nodes were calculated using the shear moduli, G_0, at small strain level shown in Fig. 11, while reduced shear moduli estimated from the back-analysis of the static load test mentioned in the previous section were used for estimation of the soil springs at the pile nodes. For the estimation of the Young's modulus of an equivalent pier and soil springs at the equivalent pier nodes, it was found that the use of soil moduli, G_0, at small strain level leads to the calculated results that match well with the measurement values. This may be due to a fact that the cross sectional area of the soil in the equivalent pier in this case is about 90% of the total area, so the soil area of disturbance zone around the pile is much smaller than the non-disturbance zone. On the other hand, for the analysis using PRABS, stiffness values of the pile springs were calculated based on the back analysis result of the vertical pile load test shown in Fig. 15.

Figure 17 shows a side view of the building. In the modelling of the foundation structure, the raft was modelled by combination of thin plates and beams. The raft base was located at 6.5 m below the original ground surface. In the analysis, the construction of the superstructure was divided into two stages in which the foundation acted as a pile group and as a piled raft. The hatching indicates the area of the superstructure constructed in the stage of piled raft.

Figure 18 shows the time histories of the total load from the building and measured water pressure beneath the raft. The construction of the building was completed in September 2004. The raft (mat slab of the basement floor) was completed at the end of December 2003. Hence the foundation was regarded as a pile group until the end of December 2003, and was regarded as a piled raft after that.

The raft base was located at 6.5 m below the original ground surface. The original ground water table (3.0 m below the ground level) was lowered to 7.5 m below the ground level until the end of February 2004, by means of deep wells. Then, the lowered ground water table was recovered to the original water table. The measured increase in the water pressure of 35 kPa corresponded to this recovery of the ground water table.

In the deformation analysis of the whole structure, rigidity of the superstructure was neglected and vertical loads from the superstructure were directly applied on the raft nodes. Figure 19 shows the distributions of loads on the raft. In the analysis using PRAB with the equivalent pier concept, the loads acting on the top of the piles, which were modelled as an equivalent pier, were summed up and placed on the top of the equivalent pier node. In analysis for the stage of pile group foundation, load increments shown in Fig. 19(a) were applied, while in analysis for the stage of piled raft foundation, load increments of Fig. 19(b) were applied on the raft. Note here that the ground water level was recovered at the construction stage of the piled raft as mentioned earlier. The buoyancy force due to the water pressure at the raft base was also taken into account in addition to the load increments of Fig. 19(b).

Figures 20 and 21 show the distributions of calculated and measured settlements of the raft in the x-direction at $y = 40.5$ m (*see* Figs. 10 and 16, section A-A′) and those in the y-direction at $x = 34.8$ m (*see* Figs. 10 and 16, section B-B′), respectively. Increment of settlements in stage of pile group are shown in Figs. 20(a) and 21(a), those in stage of piled raft are shown in Figs. 20(b) and 21(b), and the total settlements at the final construction stage are shown in Figs. 20(c) and 21(c). In the figures, the calcu-

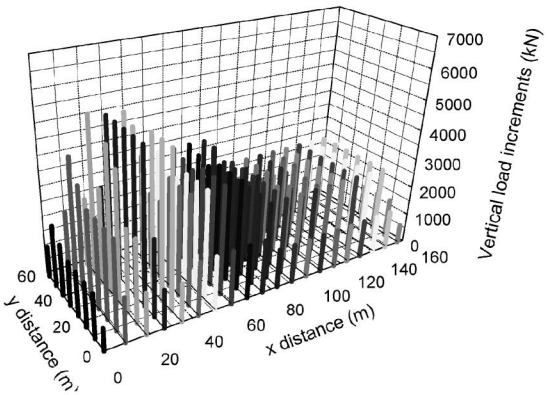

(a) Superstructure load increments in stage of pile group

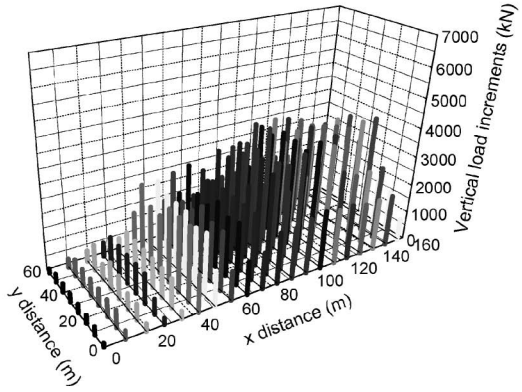

(b) Superstructure load increments in stage of piled raft

Fig. 19. Distribution of loads on the raft

lated results of Sonoda et al. (2009) in which each of the piles was modelled as a series of beam elements in the analysis using PRAB are also shown. It is seen from the figure that although the analysis tends to overestimate the measured settlements in the stage of pile group foundation and underestimate the measured settlements in the stage of piled raft foundation, the analysis predicted the measured total settlements fairly well. It can be seen from analysis results that the analysis results using PRABS match very well with the analysis results of Sonoda et al. (2009) and the analysis results using the equivalent pier concept. This demonstrates the validity of PRABS and the method to model several piles in the piled raft as the equivalent piers. Note that the calculation time using PRAB with the equivalent pier concept is less than 1/3 of the calculation time used in Sonoda et al. (2009), and the calculation time using PRABS is much less than the calculation time using PRAB.

Moreover, the distributions of calculated and measured total settlements of the raft are shown in Fig. 22(a) for the distributions of settlements in the x-direction at $y = 16.2$ m, and in Fig. 22(b) for distributions of settlements in the y-direction at $x = 132.0$ m. It is seen again from the figures that there are good agreements between the analysis results and the measured settlements.

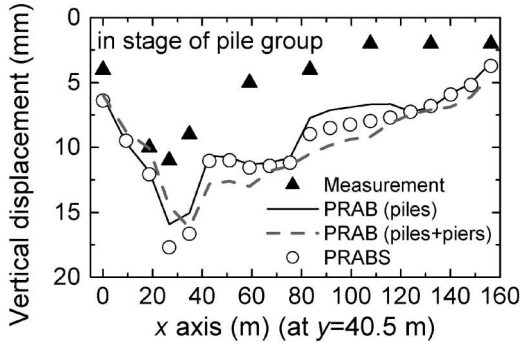

(a) Increments of settlements in stage of pile group

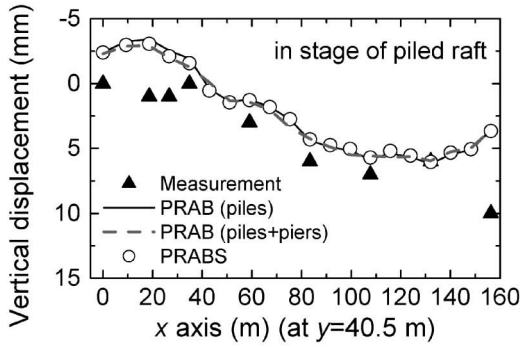

(b) Increments of settlements in stage of piled raft

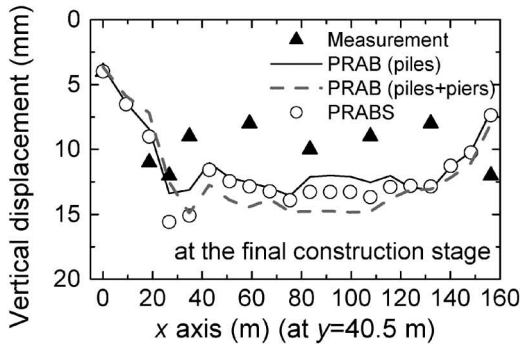

(c) Total settlements at the final construction stage

Fig. 20. Calculated and measured settlements (at $y = 40.5$ m)

CONCLUDING REMARKS

This paper presents an approximate method of analysis of piled raft foundation in which the raft is modelled as a thin plate and the piles and the soil are treated as interactive springs. The method makes it possible to solve problems of large non-uniformly arranged piled rafts in a time-saving way using a PC. The method is implemented via the computer program PRABS. Moreover, the equivalent pier concept is presented.

From the parametric study on the interaction factors and comparison between the existing solutions and those from PRABS indicate that the proposed approximate method can provide solutions of acceptable accuracy for the foundation with L/D less than 25 and s/D more than 3 which are common for piled raft foundation employed

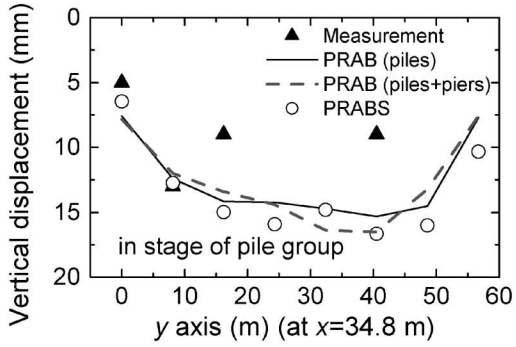

(a) Increments of settlements in stage of pile group

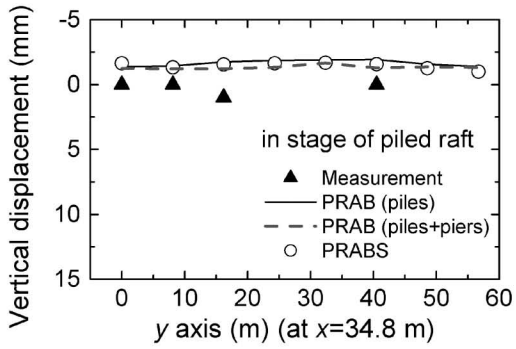

(b) Increments of settlements in stage of piled raft

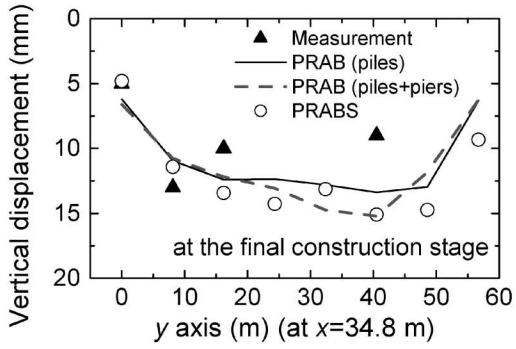

(c) Total settlements at the final construction stage

Fig. 21. Calculated and measured settlements (at $x = 34.8$ m)

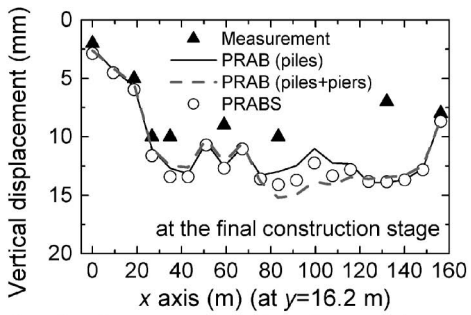

(a) Calculated and measured total settlements (at $y = 16.2$ m)

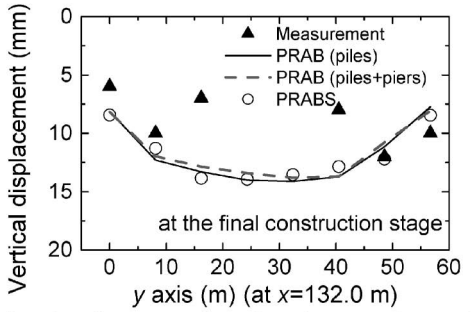

(b) Calculated and measured total settlements (at $x = 132.0$ m)

Fig. 22. Calculated and measured total settlements

in practice.

A case study demonstrates that the analysis using PRABS and PRAB with the equivalent pier concept can predict reasonably well the settlements of a full-scale piled raft containing a large number of piles and the calculation time of the analysis are less than the calculation time of the full model analysis.

ACKNOWLEDGEMENTS

The authors deeply thank Kyushu Railway Company and Kagoshima Terminal Building Corporation and Yasui Architects & Engineers, Inc. for their permission to use the valuable field measurement data.

REFERENCES

1) Anagnostopoulos, C. and Georgiadis, M. (1998): A simple analysis of piled raft foundations, *Geotechnical Engineering Journal*, **29**(1), 71–83.
2) Burland, J. B., Broms, B. B. and De Mello, V. F. B. (1977): Behaviour of foundations and structures, *Proc. 9th Int. Conf. on SMFE*, Tokyo, Japan, **2**, 496–546.
3) Fraser, R. A. and Wardle, L. J. (1976): Numerical analysis of rectangular rafts on layered foundations, *Géotechnique*, **26**(4), 613–630.
4) Hain, S. J. and Lee, I. K. (1978): The analysis of flexible pile-raft systems, *Géotechnique*, **28**(1), 65–83.
5) Harr, M. E. (1966): *Foundations of Theoretical Soil Mechanics*, McGraw-Hill, New York.
6) Horikoshi, K. and Randolph, M. F. (1999): Estimation of overall settlement of piled rafts, *Soils and Foundations*, **39**(2), 59–68.
7) Kakurai, M. (2003): Study on vertical load transfer of piles, *Dr. Thesis*, Tokyo Institute of Technology, 304 (in Japanese).
8) Kim, K. N., Lee, S. H., Kim, K. S., Chung, C. K., Kim, M. M. and Lee, H. S. (2001): Optimal pile arrangement for minimizing differential settlements in piled raft foundations, *Computers and Geotechnics*, **28**, 235–253.
9) Kitiyodom, P. and Matsumoto, T. (2002): A simplified analysis method for piled raft and pile group foundations with batter piles, *International Journal for Numerical and Analytical Methods in Geomechanics*, **26**, 1349–1369.
10) Kitiyodom, P. and Matsumoto, T. (2003): A simplified analysis method for piled raft foundations in non-homogeneous soils, *International Journal for Numerical and Analytical Methods in Geomechanics*, **27**, 85–109.
11) Kitiyodom, P., Matsumoto, T. and Kawaguchi, K. (2005): A simplified analysis method for piled raft foundations subjected to ground movements induced by tunnelling, *International Journal for Numerical and Analytical Methods in Geomechanics*, **29**, 1485–1507.
12) Mindlin, R. D. (1936): Force at a point in the interior of a semi-infinite solid, *Physics*, **7**, 195–202.
13) Poulos, H. G. and Davis, E. H. (1980): *Pile Ffoundation Analysis*

and Design, Wiley, New York.
14) Poulos, H. G. (1994): An approximate numerical analysis of pile-raft interaction, *International Journal for Numerical and Analytical Methods in Geomechanics*, **18**, 73–92.
15) Randolph, M. F. and Wroth, C. P. (1978): Analysis of deformation of vertically loaded piles, *Journal of Geotechnical Engineering Division*, ASCE, **104**(GT12), 1465–1488.
16) Randolph, M. F. and Clancy, P. (1993): Efficient design of piled rafts, *Proc. Deep Foundation on Bored and Auger Piles*, Ghent, Belgium, 119–130.
17) Randolph, M. F. (1994): Design methods for pile group and piled rafts, *Proc. 13th Int. Conf. on SMFE*, New Delhi, India, **5**, 61–82.
18) Russo, G. (1998): Numerical analysis of piled rafts, *International Journal for Numerical and Analytical Methods in Geomechanics*, **22**, 477–493.
19) Sonoda, R., Matsumoto, T., Kitiyodoom, P., Moritaka, H. and Ono, T. (2009): Case study of a piled raft foundation constructed using a reverse construction method and its post-analysis, *Canadian Geotechnical Journal*, **46**(2), 142–159.
20) Yamashita, K., Yamada, T. and Kakurai, M. (1998): Method for analysis piled raft foundations, *Proc. Deep Foundation on Bored and Auger Piles*, Ghent, Belgium, 457–464.